【 ORIGINAL ARTICLE 】

Effects of Canagliflozin on Hepatic Steatosis, Visceral Fat and Skeletal Muscle among Patients with Type 2 Diabetes and Non-alcoholic Fatty Liver Disease

Noriko Nishimiya[1], Kazuki Tajima[2], Kento Imajo[3], Akiko Kameda[2], Eiko Yoshida[2],
Yu Togashi[2], Kazutaka Aoki[4], Tomio Inoue[1], Atsushi Nakajima[3],
Daisuke Utsunomiya[1] and Yasuo Terauchi[2]

Abstract:

Objective　We assessed the effect of canagliflozin, an sodium-glucose co-transporter type-2 inhibitor, on hepatic steatosis using three imaging modalities: magnetic resonance imaging (MRI), computed tomography, and transient elastography. We further determined factors associated with improving hepatic steatosis by canagliflozin among patients with type 2 diabetes and non-alcoholic fatty liver disease (NAFLD).

Methods　We conducted a six-month prospective single-arm study between August 2015 and June 2017. The primary outcome was the change in hepatic steatosis assessed using the hepatic proton density fat fraction (PDFF) on MRI before and after treatment with canagliflozin. The secondary outcomes were changes in measures of glucose metabolism, including the hepatic glucose uptake on fluorodeoxyglucose-positron emission tomography, and the inflammation and volumes of visceral and subcutaneous adipose tissue and skeletal muscle.

Patients　Nine patients with type 2 diabetes and NAFLD completed this study. All participants received canagliflozin at a dose of 100 mg daily.

Results　Canagliflozin caused a significant reduction in hepatic PDFF from baseline [median 20.6% (interquartile range 11.7%, 29.8%)] after 6 months [10.6% (5.4%, 22.6%), p=0.008]. Canagliflozin also significantly reduced the body weight, glycated hemoglobin, homeostasis model assessment of insulin resistance (HOMA-IR), high sensitivity C-reactive protein (hs-CRP), and volumes of adipose tissue and skeletal muscle (all p<0.05). The reduction in hepatic PDFF was not correlated with changes in the body weight, HOMA-IR, hs-CRP, or volume of adipose tissue and skeletal muscle from baseline after six months.

Conclusion　Among patients with type 2 diabetes and NAFLD, canagliflozin improved hepatic steatosis. The effect may be independent of reducing adiposity, insulin resistance, inflammation, and skeletal muscle volume.

Key words: sodium-glucose co-transporter type-2 (SGLT2) inhibitor, non-alcoholic fatty liver disease, imaging, adipose tissue, skeletal muscle

(Intern Med 60: 3391-3399, 2021)
(DOI: 10.2169/internalmedicine.7134-21)

Introduction

The prevalence of non-alcoholic fatty liver disease (NAFLD) has been increasing worldwide due to the obesity epidemic (1-3). NAFLD affects 75% of patients with type 2 diabetes, and up to 30% of NAFLD patients develop nonalcoholic steatohepatitis (NASH), liver cirrhosis, and hepatocellular carcinoma (4, 5). Therefore, preventing the progression of NAFLD to NASH in patients with type 2 diabetes is a pressing need.

Sodium-glucose co-transporter type-2 (SGLT2) inhibitors reduce blood glucose levels by promoting glucose excretion in the urine and have been shown to improve cardiovascular and renal outcomes among patients with type 2 diabetes (6-8). SGLT2 inhibitors also improve adiposity, blood liver enzyme levels, and hepatic steatosis and fibrosis among patients with type 2 diabetes and NAFLD. Recent prospective studies have demonstrated the histological improvement in steatosis and fibrosis associated with glucose metabolism by an SGLT2 inhibitor (9, 10). The potential mechanisms by which SGLT2 inhibitors improve hepatic steatosis include reducing body weight, visceral fat, and lean body mass (11, 12) and improving insulin resistance and inflammation (13). However, no studies have comprehensively assessed these factors and evaluated the individual association with improving hepatic steatosis. Filling the knowledge gaps may facilitate the development of targeted therapies for NAFLD among patients with type 2 diabetes.

We designed a six-month prospective single-arm study to assess the effect of canagliflozin on hepatic steatosis using magnetic resonance imaging (MRI), computed tomography (CT) imaging, and transient elastography among patients with type 2 diabetes and NAFLD. We also measured the adiposity and assessed the glucose metabolism, including the hepatic glucose uptake, as well as the inflammation and skeletal muscle area before and after treatment with canagliflozin. We then determined the factors associated with the improvement of hepatic steatosis by canagliflozin.

Materials and Methods

Study design and patients

This study was conducted at Yokohama City University (Yokohama, Japan) between August 2015 and June 2017. This study complied with the ethical principles of the Declaration of Helsinki and was approved by the Ethics Committee of Yokohama City University Hospital. This study is registered in the UMIN Clinical Trials Registry (UMIN 000018814). Written informed consent was obtained from all participants.

Patients were eligible if they were between 20 and 64 years old and had type 2 diabetes with a glycated hemoglobin (HbA1c) level of 6.5% to 9.0%. They were required to have a body mass index (BMI) greater than 20 kg/m^2 and

NAFLD, which was defined as the presence of hepatic steatosis documented by imaging or histology in the absence of secondary causes of hepatic fat accumulation (14). Patients were excluded if they had intolerance to SGLT inhibitors; severe ketosis or diabetic coma; infection; a perioperative state; trauma; a history of liver disease (except for NAFLD), renal disease, mental disorder, or cancer; difficulty undergoing image examinations or analyses; and contraindications for MRI. Women who were pregnant or lactating were also excluded.

All patients received canagliflozin (100 mg orally once daily in the morning) until study completion. They continued to take other glucose-lowering therapies, but the doses were allowed to be adjusted as required to minimize the risk of hypoglycemia or hyperglycemia.

Clinical and biochemical analyses

Patients were evaluated at baseline and one, three, and six months after receiving canagliflozin, with a focus on assessing glucose and lipid parameters, the hepatic function, and the body weight, height, waist circumference, and systolic and diastolic blood pressures. Glucose parameters included fasting plasma glucose and HbA1c, and lipid parameters included triglycerides, high-density lipoprotein, and low-density lipoprotein cholesterol. The assessments of the hepatic function included measuring the aspartate aminotransferase (AST), alanine aminotransferase (ALT), and gamma-glutamyl transpeptidase (γ-GTP) levels.

At baseline and the six-month follow-up, we collected additional data, including measurements of the insulin, adiponectin, leptin, free fatty acid, high-sensitivity C-reactive protein (hs-CRP), tumor necrosis factor-α, plasminogen activator inhibitor-1, ferritin, type IV collagen, urinary albumin, and creatinine excretion. The homeostasis model assessment of insulin resistance (HOMA-IR) was calculated as (fasting plasma glucose×insulin)/405 (15), and the fibrosis-4 index was calculated as $(age \times AST)/(Plt~(10^9/L) \times \sqrt{ALT})$. We calculated the estimated glomerular filtration rate (eGFR) according to the following equation: $194 \times Cre^{-1.094} \times age^{-0.287}$ for men and $194 \times Cre^{-1.094} \times age^{-0.287} \times 0.739$ for women (16).

The quantitative assessment of hepatic steatosis

At baseline and the six-month follow-up, hepatic steatosis was evaluated using MRI, CT, and transient elastography imaging. The primary outcome was the change in the hepatic proton density fat fraction (PDFF) on MRI before and after treatment with canagliflozin. Hepatic MRI was performed using a 3.0-T MRI system (Discovery MR750w; GE Healthcare, Milwaukee, USA) with the anterior array coil. The hepatic PDFF was calculated using the chemical shift-based multipoint water-fat separation method with phase correction and the iterative decomposition of water and fat with echo asymmetry and least-squares estimation (IDEAL-IQ; GE Healthcare) method (17-19). The parameters of the sequence were as follows: repetition time, 6.63 ms; echo time, Min0.9 ms-Max4.8 ms (6 echo); flip angle, 1°;

sensitivity-encoding factor, 2.5 (phase); field of view, 440× 352 mm; acquisition matrix 160×160; and reconstructive voxel size, 2.8×2.8×2.8 mm. Quantification of the hepatic PDFF was performed by an experienced radiologist based on 3 regions of interest (ROIs) of 300 mm^2 within the right hepatic lobe parenchyma at the middle level of the liver [20]. The average PDFF for all ROIs was used for the analyses.

Unenhanced CT was performed using a 128-section multidetector scanner (SOMATOM Definition AS+; Siemens, Munich, Germany) with the following parameters: 120 kVp using an automatic exposure control system, collimation of 0.6 mm×128, section thickness of 5 mm. Three ROIs were drawn on the right hepatic lobe in the same way as for the PDFF analysis. The mean CT values in Hounsfield units (HU) of all ROIs was used for the analyses.

The ultrasound-based controlled attenuation parameter (CAP) value was measured using transient elastography (M-probe, Fibroscan; EchoSens, Paris, France) by an experienced hepatologist [21]. The CAP is determined only for validated measurements according to the same criteria used for liver stiffness measurement (LSM) and on the same signals, ensuring that the liver ultrasonic attenuation is obtained simultaneously and in the same volume of liver parenchyma as the LSM. The final CAP value, which ranges from 100 to 400 decibels per meter (dB/m), is the median of individual measurements. As an indicator of variability, the ratio of the interquartile range (IQR) of CAP values to the median (IQR/MCAP) was calculated.

To assess the severity of NAFLD, the 'NASH, ferritin, insulin, type IV collagen 7S' (NAFIC) score [22] was calculated for each participant.

The quantitative assessment of hepatic stiffness

At baseline and the six-month follow-up, magnetic resonance (MR) elastography was performed using the 3.0-T MRI system. Continuous longitudinal mechanical waves (60 Hz) were generated using a passive acoustic driver placed against the anterior chest wall. A two-dimensional spin-echo planar MR elastography sequence was used to acquire axial wave images using the following parameters: repetition time/echo time: 50/23 ms; continuous sinusoidal vibration: 60 Hz; FOV: 32-42 cm; matrix size: 256×64; flip angle: 30°; section thickness: 10 mm; 4 evenly spaced phase offsets; and 4 pairs of 60-Hz trapezoidal motion encoding gradients with zeroth and first moment nulling along the through-plane direction. All processing steps were applied automatically, without manual intervention, to yield quantitative images of tissue shear stiffness in kilopascals [20]. The hepatic liver stiffness was analyzed by one experienced hepatologist. ROIs were drawn at each of the four slice locations in portions of the liver in which the corresponding wave images showed clearly observable wave propagation, avoiding liver edges, large blood vessels, and artifacts [23]. The average liver stiffness for all ROIs was used for the analyses.

Liver stiffness was also evaluated using transient elastography (M-probe, Fibroscan; EchoSens) by an experienced hepatologist. Transient elastography-based LSM were calculated according to the previously described method [21]. The median liver stiffness value was considered representative of the elastic modulus of the liver. As an indicator of variability, the ratio of the IQR of liver stiffness to the median (IQR/Median) was calculated. The unreliability of the LSM was defined as an IQR/Median >30%, and technical failure was defined by an inability to obtain 10 valid measurements.

The quantitative assessment of the hepatic glucose uptake

The hepatic glucose uptake was quantified using 2-deoxy-2-[fluorine-18] fluoro-D-glucose integrated positron emission tomography with CT (^{18}F-FDG-PET/CT) with a whole-body PET/CT scanner (Celesteion; Canon Medical Systems, Otawara, Japan) equipped with 16 rows of CT detectors. FDG at a dose of 3.7 MBq/kg (upper limit of 370 MBq) was intravenously administered under a fasting state of >6 hours. After a 60-minute resting period following administration, FDG-PET/CT was performed. First, low-dose CT was performed with a tube voltage of 120 kVp using an automatic exposure control system with an upper limit of 80 mAs, a beam pitch of 0.938, and a 16-row detector mode with 2-mm section thickness [19]. PET was then performed using a three-dimensional mode. The emission scan time per bed position was 120 seconds, and 12-14 bed positions were acquired. Three ROIs were drawn in the right hepatic lobe, and the mean standardized uptake value (SUV$_{mean}$) of all ROIs was used for the analyses as the hepatic SUV$_{mean}$.

The quantitative assessments of the visceral and subcutaneous adipose tissue and skeletal muscle

At baseline and six-month follow-up, the cross-sectional areas of visceral adipose tissue and subcutaneous adipose tissue were quantified at both the umbilical and third lumbar vertebral (L3) levels using a dedicated workstation (SYNAPSE VINCENT; Fuji Medical Systems, Tokyo, Japan). The adipose tissue was defined as the region with a CT attenuation of -200 to -50 HU. We also quantified the cross-sectional areas of the total skeletal muscle with free-hand ROIs at the L3 vertebral level and calculated the skeletal muscle index as the cross-sectional areas of the total skeletal muscle divided by the square of the body height (cm^2/m^2) [24-26]. The areas of the total skeletal muscle with a CT attenuation of -200 to 0 HU were defined as the intermuscular adipose tissue, and those with a CT attenuation of 0 to 150 HU were defined as the muscle parenchyma. We also calculated the proportion of the intermuscular adipose tissue and muscle parenchyma divided by the total skeletal muscle at the L3 vertebral level.

Study endpoints

The primary endpoint was the change in hepatic steatosis assessed using PDFF on MRI after treatment with canagli-
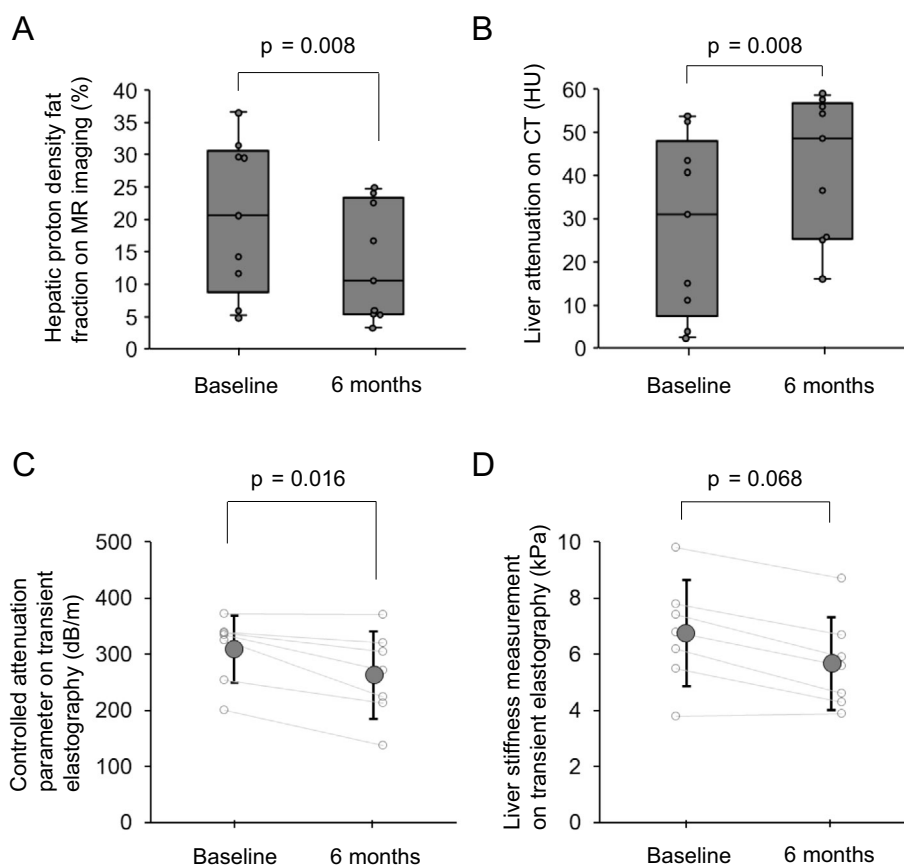
Figure. **Hepatic steatosis and fibrosis at baseline and 6 months after treatment with canagliflozin 100 mg. (A) Hepatic proton density fat fraction on MRI; n=9. (B) Liver attenuation on CT; n=9. (C) Controlled attenuation parameter on transient elastography; n=7. (D) Liver stiffness measurement on transient elastography; n=7. Non-parametric data are shown in box plots, and parametric data are shown as the mean±SD in line graphs. Data at baseline and 6 months after treatment with canagliflozin 100 mg were compared using a paired t-test or Wilcoxon's signed-rank test, as appropriate. Two participants had incomplete imaging findings for ultrasound-based controlled attenuation parameters and liver stiffness measurements on transient elastography.**

flozin. The secondary endpoints were the differences in the changes between baseline and six months of the treatment in the following variables: liver attenuation on CT, CAP and liver stiffness measurement on transient elastography, visceral and subcutaneous adipose tissue volume at the L3 vertebral and umbilical levels, skeletal muscle area at the L3 vertebral level, proportion of muscle parenchyma and intermuscular adipose tissue in skeletal muscle at the L3 vertebral level, the hepatic FDG uptake, insulin, ferritin, type IV collagen 7S, NAFIC score, fibrosis-4 index, fasting plasma glucose, HbA1c, HOMA-IR, uric acid, AST, ALT, γ-GTP, triglycerides, high-density lipoprotein, and low-density lipoprotein cholesterol, adiponectin, leptin, free fatty acid, hs-CRP, tumor necrosis factor-α, plasminogen activator inhibitor-1, urinary albumin, creatinine excretion, eGFR, hemoglobin, hematocrit, body weight, height, waist circumference, and systolic and diastolic blood pressures. We further determined the associations of the change in the hepatic PDFF on MRI with changes in the clinical and imaging parameters.

Sample size

No previous studies have evaluated the effect of SGLT2 inhibitors on hepatic steatosis on MRI. Based on the findings from another study assessing the effect of the glucose-lowering agent thiazolidine on hepatic fat content on MRI (27), we determined a sample size of 20 to be necessary in our single-arm study. When we performed a power analysis later, the minimum number of subjects required was determined to be eight. Therefore, we finished this study before enrolling 20 subjects.

The safety and evaluation of adverse events

During the study, the investigators regularly monitored the appearance of any hypoglycemic symptoms and signs as well as all other adverse events (AEs) through regular medical checkups. AEs data and vital signs were collected at each study visit.

Statistical analyses

Descriptive statistics are presented as the means and stan-

Table 1. Clinical Characteristics at Baseline, and 1 Month, 3 Months, and 6 Months after Treatment with Canagliflozin 100 mg.

	Baseline	1 month	3 months	6 months
Age (years)	50 (43.0, 60.0)	-	-	-
Male / Female (n)	4/5	-	-	-
Body weight (kg)	72.4 (59.9, 73.0)	70.5 (58.5, 72.6)*	68.7 (58.3, 70.4)*	69.3 (59.6, 70.4)*
Body mass index (kg/m^2)	27.3 (24.7, 29.3)	26.4 (24.7, 28.7)*	26.0 (24.6, 28.7)*	25.4 (24.2, 27.7)*
Waist circumference (cm)	96.5 (92,102)	96 (89, 101)	96.5 (91, 101)	93 (88, 98)*
Systolic blood pressure (mmHg)	147.3±12.0	137.7±12.7	130.6±4.5**	133.2±12.8*
Diastolic blood pressure (mmHg)	91.0±8.9	84. 6±9.7	83.8±7.9	85.1±8.1
HbA1c (%)	7.50±0.71	7.07±0.50**	6.74±0.45*	6.71±0.52*
Fasting plasma glucose (mg/dL)	153.7±19.6	137.0±14.8*	128.0±18.5*	124.3±21.0*
Insulin (μU/mL)	22.4 (16.4, 28.1)	N/A	N/A	13.4 (10.9, 19.3)*
Glucose-lowering therapy				
Biganide (n)	9	9	9	9
DPP4 inhibitor (n)	4	4	4	4
Sulfonylurea (n)	2	2	2	2
α-Glucosidase inhibitor (n)	1	1	1	1
Glinide (n)	0	0	0	0
Thiazolidine (n)	0	0	0	0
GLP-1 analogue (n)	0	0	0	0
Insulin (n)	0	0	0	0
Adiponectin (μg/mL)	4.8 (4.0, 6.8)	N/A	N/A	5.4 (4.0, 8.0)
Leptin (ng/mL)	12.7 (8.2, 25.6)	N/A	N/A	11.9 (10.3, 14.9)
HOMA-IR	9.48 (6.50, 10.86)	N/A	N/A	4.42 (2.91, 5.86)**
Triglycerides (mg/dL)	161 (96, 203)	134 (115, 221)	123 (79, 152)	102 (86, 141)
HDL cholesterol (mg/dL)	53.0±9.8	50.5±8.9	55.0±9.6	56.4±10.6
LDL cholesterol (mg/dL)	95.5±22.2	94.8±26.5	99.3±26.0	99.6±18.4
Free fatty acid (mmol/L)	630 (560, 720)	N/A	N/A	630(490, 930)
Aspartate aminotransferase (U/L)	25 (23, 56)	26 (21, 37)	23 (19, 38)	26 (17, 38)
Alanine aminotransferase (U/L)	39 (23, 69)	37 (20, 46)	21 (19, 55)	21 (15, 54)
Gamma-glutamyl transpeptidase (U/L)	40 (37, 61)	36 (22, 61)*	31 (22, 48)*	27 (21, 35)
Ferritin (ng/dL)	198 (145, 210)	N/A	N/A	92 (72, 169)**
Type IV collagen 7S (ng/dL)	5.5±0.9	N/A	N/A	4.9±0.4*
Fibrosis-4 index	0.92 (0.70, 1.63)	0.85 (0.76, 1.28)	0.78 (0.65, 1.27)	0.77 (0.68, 1.14)
NAFIC score	3 (2, 3)	N/A	N/A	2 (1, 3)
Estimated glomerular filtration rate (mL/min/1.73m^2)	103.2±18.8	91.0±17.7*	91.9±15.9**	98.4±20.1
Uric acid (mg/dL)	5.2±1.4	4.3±1.0**	4.5±1.0*	4.5±1.1*
Urinary albumin-creatinine ratio (mg/gCr)	12.1 (9.4, 14.9)	N/A	N/A	9.5 (7.8, 14.2)
Hemoglobin (g/dL)	14.5±1.1	14.8±1.1	15.0±1.0*	15.1±0.9
Hematocrit (%)	43.3±3.2	44.0±3.2	44.8±3.0	44.9±3.0
hs-CRP (mg/dL)	0.11 (0.07,0.27)	N/A	N/A	0.09 (0.06,0.16)*
Tumor necrosis factor-α (pg/mL)	0.96±0.24	N/A	N/A	0.98±0.24
Plasminogen activator inhibitor-1 (ng/mL)	41 (37, 46)	N/A	N/A	26 (17, 35)
Hepatic SUV$_{mean}$ on ^{18}F-FDG-PET/CT	2.34±0.27	N/A	N/A	2.27±0.41

Data are presented as the mean and standard deviation (SD), median (25th to 75th percentile), or proportions, as appropriate. Clinical parameters before and 6 months after treatment with canagliflozin 100 mg were compared using paired t-test or the Wilcoxon signed-rank test. The repeated measures ANOVA or the Friedman test followed by post hoc paired t-test or the Wilcoxon singed-rank test with Bonferroni correction was used to compare clinical parameters values at 1 month, 3 months, and 6 months after treatment, respectively, compared to the baseline value. n=9. *$p<0.05$, **$p<0.01$ vs. baseline value. N/A: not applicable

dard deviation (SD), median (25th to 75th percentile), or proportions where appropriate. Clinical parameters before and 6 months after treatment with canagliflozin 100 mg were compared using a paired t-test or Wilcoxon's signed-rank test, as appropriate. A repeated measures analysis of variance or the Friedman test followed by a post hoc paired t-test or Wilcoxon's singed-rank test with Bonferroni correction was used to compare clinical parameters values at one, three, and six months after treatment compared to the base-line value. The associations between the individual parameter were calculated using Spearman's correlation coefficients.

Statistical analyses were performed for the data presented in Figure and Tables 1 and 2 by Kondo Photo Process (Osaka, Japan), using the IBM SPSS Statistics 22.0 software program (International Business Machines, Armonk, USA; and MedCalc version 17.2; MedCalc, Mariakerke, Belgium). The data in Table 3 were statically analyzed by the authors

Table 2. Adipose Tissue and Skeletal Muscle Volumes at Baseline and 6 Months after Treatment with Canagliflozin 100 mg.

	Baseline	6 months
Visceral adipose tissue (umbilical level) (cm^2)	167 (112, 195)	152 (96, 173)**
Visceral adipose tissue (L3 vertebral level) (cm^2)	183 (132, 206)	141(103, 193)*
Subcutaneous adipose tissue (umbilical level) (cm^2)	207 (121, 234)	184 (126, 254)
Subcutaneous adipose tissue (L3 vertebral level) (cm^2)	164 (130, 209)	129 (112, 186)*
Skeletal muscle (L3 vertebral level) (cm^2)	124.6 (100.8, 133.0)	119.7 (98.8, 125.5)*
Skeletal muscle index (L3 vertebral level) (cm^2/m^2)	47.7 (40.9, 50.6)	44.5 (41.6, 47.6)*
Proportion of muscle parenchyma within skeletal muscle (%)	77.9±10.1	78.6±10.5
Proportion of intermuscular adipose tissue within skeletal muscle (%)	22.3 (13.2, 29.1)	21.6 (11.3, 30.4)

Data are presented as the mean and standard deviation for normally distributed variables and median (25th to 75th) percentile for variables with skewed distribution. Data before and 6 months after treatment with canagliflozin 100 mg were compared using paired *t*-test or the Wilcoxon signed-rank test. *p<0.05, **p<0.01 vs. baseline value.

using the JMP software program (version 12.2.0; SAS Institute, Cary, USA). Statistical significance was defined by a two-sided p value <0.05.

Results

Of the 10 participants enrolled in the current study, we excluded 1 who violated our study protocol, leaving a final analytical sample size of 9 participants (Table 1). Of the 9 participants, 5 (56%) were women, the median (25th to 75th percentile) age was 50.0 (43.0, 60.0) years old, and the mean (SD) HbA1c value was 7.5% (0.7%). Table 1 shows the clinical and biochemical data at baseline and the one-, three-, and six-month follow-up exams. Canagliflozin 100 mg induced a significant reduction in body weight, BMI, fasting plasma glucose and HbA1c, and uric acid at one, three, and six months after treatment. There was a significant reduction in the waist circumference, insulin, HOMA-IR, ferritin, type IV collagen 7S, and hs-CRP from baseline after six months. In this study, we measured the hepatic SUV$_{mean}$ to evaluate the glucose uptake in the liver. Canagliflozin induced no change in the hepatic SUV$_{mean}$ from baseline at six months.

Two participants had incomplete imaging findings regarding the ultrasound-based controlled attenuation parameters and liver stiffness measurements on transient elastography due to the obtained unreliable data. Canagliflozin 100 mg caused a significant reduction in the hepatic PDFF on MRI and in the ultrasound-based controlled attenuation parameter on transient elastography and increased the liver attenuation on CT from baseline at 6 months (Figure A-C). There were no significant changes in the liver stiffness on transient elastography from baseline after six months (Figure D).

Canagliflozin 100 mg induced a significant reduction in the subcutaneous and visceral adipose tissue volumes at the L3 vertebral level from baseline after 6 months (Table 2). The skeletal muscle volume at the L3 vertebral level was decreased from baseline after six months, whereas the proportion of the muscle parenchyma and intermuscular adipose tissue within the total skeletal muscle remained unchanged.

The reduction in hepatic PDFF on MRI was significantly correlated with the increase in hepatic CT attenuation (Spearman's correlation coefficient: -0.88) and changes in the circulating levels of leptin and triglycerides (Table 3) from baseline after 6 months. The reduction in hepatic PDFF on MRI was not correlated with the changes in the body weight, BMI, waist circumference, HOMA-IR, hs-CRP, subcutaneous and visceral adipose tissue volumes, or skeletal muscle volume from baseline after six months.

No adverse events, such as hypoglycemia, dehydration, or urinary tract infection, were noted during this study.

Discussion

In this 6-month prospective single-arm study, canagliflozin 100 mg daily had significant effects on reducing the values of fasting plasma glucose, HbA1c, insulin resistance, inflammation, systolic blood pressure, and circulating uric acid and ferritin among patients with type 2 diabetes and NAFLD. Canagliflozin also had significant effects on reducing hepatic steatosis, subcutaneous and visceral adipose tissue volumes at the L3 vertebral level, and the skeletal muscle volume. The reduction in hepatic steatosis assessed using hepatic PDFF on MRI was not correlated with changes in adiposity, insulin resistance, inflammation, or skeletal muscle volume by canagliflozin.

In a meta-analysis including 6 randomized controlled trials of SGLT2 inhibitors in patients with type 2 diabetes and NAFLD (n=309), SGLT2 inhibitors reduced hepatic steatosis assessed using hepatic PDFF on MRI [weight mean difference -2.07%, 95% confidence interval (CI) -3.86, -0.28%, p =0.02], body weight (weight mean difference -1.62 kg, 95% CI -2.02, -1.23 kg, p<0.00001), and visceral fat volume (weight mean difference -19.98 cm^2, 95% CI -27.18, -12.798 cm^2, p<0.00001, respectively) compared to those not taking SGLT2 inhibitors (28). The current study expands on this knowledge by demonstrating that canagliflozin improved hepatic steatosis but not hepatic stiffness on three imaging modalities among patients with type 2 diabetes and NAFLD. However, the long-term (≥6 months) effects of SGLT2 in-

Table 3. Associations of Change in Hepatic Proton Density Fat Fraction on MR Imaging with Changes in Other Clinical and Imaging Parameters.

	Spearman's correlation coefficients	p values
Δ Body weight (kg)	0.05	0.90
Δ Body mass index (kg/m^2)	0.05	0.90
Δ Waist circumference (cm)	0.15	0.70
Δ Systolic blood pressure (mmHg)	-0.25	0.52
Δ Diastolic blood pressure (mmHg)	0.12	0.77
Δ HbA1c (%)	0.30	0.44
Δ Fasting plasma glucose (mg/dL)	-0.29	0.44
Δ Insulin (μU/mL)	0.37	0.33
Δ Adiponectin (μg/mL)	-0.10	0.80
Δ Leptin (ng/mL)	-0.68	0.04*
Δ HOMA-IR	0.20	0.61
Δ Triglycerides (mg/dL)	0.78	0.01*
Δ HDL cholesterol (mg/dL)	-0.18	0.65
Δ LDL cholesterol (mg/dL)	0.13	0.73
Δ Free fatty acid (mmol/L)	0.31	0.42
Δ Aspartate aminotransferase (U/L)	0.02	0.97
Δ Alanine aminotransferase (U/L)	0.03	0.93
Δ Gamma-glutamyl transpeptidase (U/L)	0.45	0.22
Δ Ferritin (ng/dL)	0.20	0.61
Δ Type IV collagen 7S (ng/dL)	-0.54	0.13
Δ Fibrosis-4 index	-0.05	0.90
Δ NAFIC score	0.31	0.41
Δ Estimated glomerular filtration rate (ml/min/1.73m^2)	0.20	0.61
Δ Uric acid (mg/dL)	-0.17	0.67
Δ Urinary albumin-creatinine ratio (mg/gCr)	0.02	0.97
Δ Hemoglobin (g/dL)	0.07	0.86
Δ Hematocrit (%)	0.12	0.76
Δ hs-CRP (mg/dL)	0.24	0.54
Δ Tumor necrosis factor-α (pg/mL)	0.17	0.66
Δ Plasminogen activator inhibitor-1 (ng/mL)	-0.34	0.36
Δ Hepatic CT attenuation (HU)	-0.88	0.002**
Δ Magnetic resonance elastography	-0.34	0.37
Δ Controlled attenuation parameter (dB/m)	0.14	0.76
Δ Liver stiffness measurement (kPa)	0.74	0.06
Δ Visceral adipose tissue (Umbilical level) (cm^2)	0.25	0.52
Δ Visceral adipose tissue (L3 level) (cm^2)	0.43	0.24
Δ Subcutaneous adipose tissue (Umbilical level) (cm^2)	-0.05	0.90
Δ Subcutaneous adipose tissue (L3 level) (cm^2)	-0.33	0.38
Δ Total skeletal muscle (L3 level) (cm^2)	0.29	0.44
Δ Skeletal muscle index (L3 level) (cm^2/m^2)	0.07	0.86

Spearman's correlation coefficients are shown. Changes (Δ) were calculated by subtracting the baseline value from the value 6 months after treatment with canagliflozin 100 mg. Statistical significance was defined as $p<0.05$. *$p<0.05$, **$p<0.01$.

hibitors on hepatic stiffness remain unclear.

There are several potential mechanisms that may underlie the observed effects of canagliflozin for improving hepatic steatosis. First, SGLT2 inhibitors cause energy loss by increasing urinary glucose excretion and reducing body weight and visceral fat. These changes may result in increasing β-oxidation and fat metabolism in the liver. However, the results from this study are consistent with those of previous studies demonstrating that the improvement in hepatic steatosis by SGLT2 inhibitors was independent of changes in the body weight, visceral fat mass, and glycated hemoglobin

values (29, 30). Second, SGLT2 inhibitors reduce blood glucose levels and insulin resistance (31). Improving glucose metabolism and insulin resistance downregulates the levels of carbohydrate responsive element-binding protein, a transcription factor responsible for activating fatty acid synthesis in the liver, and sterol regulatory element-binding protein 1c, a transcription factor that inhibits *de novo* lipogenesis in the liver (32, 33). However, this study suggested no correlations between changes in hepatic steatosis and changes in measures of glucose metabolism and insulin resistance. Third, SGLT2 inhibitors reduce inflammatory markers, oxidative

stress, and glucose oxidation and accelerate lipolysis and free fatty acid oxidation (13). These changes may help improve NAFLD. The present findings showed no correlation between the reduction in hepatic PDFF and changes in circulating levels of hs-CRP, tumor necrosis factor-α, or plasminogen activator inhibitor-1 by canagliflozin.

Whether or not the hepatic FDG uptake is related to the severity of hepatic steatosis is unclear. One study reported that a mild to moderate degree of fatty liver had a positive correlation with the FDG uptake in the liver, whereas a severe degree of fatty liver negatively affected the uptake (34). Some factors, such as the BMI and triglyceride and high-density lipoprotein cholesterol levels, also affect the hepatic FDG uptake (34, 35). An SGLT2 inhibitor is considered to cause an augmented hepatic glucose uptake due to a metabolic switch from glucose to fatty substrate utilization (13). In the present study, the hepatic FDG uptake was not affected by canagliflozin. Except for an improvement in hepatic steatosis, the BMI and triglyceride and high-density lipoprotein cholesterol levels may affect the uptake value.

Canagliflozin 100 mg significantly reduced the skeletal muscle volume at the L3 vertebral level over 6 months. However, the proportion of muscle parenchyma within the total skeletal muscle remained unchanged, suggesting that the decrease in skeletal muscle volume after treatment with canagliflozin may be attributable to a reduction in the plasma volume (36). Further studies are warranted to investigate whether or not the long-term use of SGLT2 inhibitors decreases skeletal muscle among patients with type 2 diabetes.

The strengths of this study include the assessments of adiposity, insulin resistance, inflammation, and skeletal muscle and hepatic steatosis using imaging modalities before and 6 months after treatment with canagliflozin 100 mg among patients with type 2 diabetes and NAFLD. However, our study was limited by its small sample size and the lack of a placebo control. Therefore, the observed changes in parameters during the study period might have been due to or influenced by factors other than canagliflozin itself, including the subjects' diet and degree of physical activity, regression to the mean, or a placebo-like effect. We observed no marked changes in the hepatic function measurements (AST and ALT) or NAFIC score, which may be a consequence of the sample size. Randomized controlled clinical trials are required to investigate whether or not canagliflozin improves hepatic outcomes among patients with type 2 diabetes and NAFLD.

In conclusion, among patients with type 2 diabetes and NAFLD, canagliflozin 100 mg had significant effects on improving circulating measures of glucose metabolism, adiposity, insulin resistance, inflammation, and hepatic steatosis. The effect of canagliflozin on hepatic steatosis may be independent of the reduction in adiposity, insulin resistance, inflammation, and skeletal muscle volume induced by canagliflozin.

References

1. Anstee QM, McPherson S, Day CP. How big a problem is nonalcoholic fatty liver disease? BMJ **343**: d3897, 2011.
2. Ratziu V, Bellentani S, Cortez-Pinto H, Day C, Marchesini G. A position statement on NAFLD/NASH based on the EASL 2009 special conference. J Hepatol **53**: 372-384, 2010.
3. Targher G, Byrne CD. Clinical review: nonalcoholic fatty liver disease: a novel cardiometabolic risk factor for type 2 diabetes and its complications. J Clin Endocrinol Metab **98**: 483-495, 2013.
4. Adams LA, Lymp JF, St Sauver J, et al. The natural history of nonalcoholic fatty liver disease: a population-based cohort study. Gastroenterology **129**: 113-121, 2005.
5. Williams CD, Stengel J, Asike MI, et al. Prevalence of nonalcoholic fatty liver disease and nonalcoholic steatohepatitis among a largely middle-aged population utilizing ultrasound and liver biopsy: a prospective study. Gastroenterology **140**: 124-131, 2011.
6. Zinman B, Wanner C, Lachin JM, et al. Empagliflozin, cardiovascular outcomes, and mortality in type 2 diabetes. N Engl J Med **373**: 2117-2128, 2015.
7. Neal B, Perkovic V, Mahaffey KW, et al. Canagliflozin and cardiovascular and renal events in type 2 diabetes. N Engl J Med **377**: 644-657, 2017.
8. Wiviott SD, Raz I, Bonaca MP, et al. Dapagliflozin and cardiovascular outcomes in type 2 diabetes. N Engl J Med **380**: 347-357, 2019.
9. Akuta N, Kawamura Y, Watanabe C, et al. Impact of sodium glucose cotransporter 2 inhibitor on histological features and glucose metabolism of non-alcoholic fatty liver disease complicated by diabetes mellitus. Hepatol Res **49**: 531-539, 2019.
10. Akuta N, Watanabe C, Kawamura Y, et al. Effects of a sodium-glucose cotransporter 2 inhibitor in nonalcoholic fatty liver disease complicated by diabetes mellitus: preliminary prospective study based on serial liver biopsies. Hepatol Commun **1**: 46-52, 2017.
11. Ohta A, Kato H, Ishii S, et al. Ipragliflozin, a sodium glucose co-

transporter 2 inhibitor, reduces intrahepatic lipid content and abdominal visceral fat volume in patients with type 2 diabetes. Expert Opin Pharmacother **18**: 1433-1438, 2017.

12. Dixon JB, Bhathal PS, Hughes NR, O'Brien PE. Nonalcoholic fatty liver disease: improvement in liver histological analysis with weight loss. Hepatology (Baltimore, Md) **39**: 1647-1654, 2004.

13. Ferrannini E, Baldi S, Frascerra S, et al. Shift to fatty substrate utilization in response to sodium-glucose cotransporter 2 inhibition in subjects without diabetes and patients with type 2 diabetes. Diabetes **65**: 1190-1195, 2016.

14. Watanabe S, Hashimoto E, Ikejima K, et al. Evidence-based clinical practice guidelines for nonalcoholic fatty liver disease/nonalcoholic steatohepatitis. J Gastroenterol **50**: 364-377, 2015.

15. Matthews DR, Hosker JP, Rudenski AS, Naylor BA, Treacher DF, Turner RC. Homeostasis model assessment: insulin resistance and beta-cell function from fasting plasma glucose and insulin concentrations in man. Diabetologia **28**: 412-419, 1985.

16. Matsuo S, Imai E, Horio M, et al. Revised equations for estimated GFR from serum creatinine in Japan. Am J Kidney Dis **53**: 982-992, 2009.

17. Idilman IS, Keskin O, Celik A, et al. A comparison of liver fat content as determined by magnetic resonance imaging-proton density fat fraction and MRS versus liver histology in non-alcoholic fatty liver disease. Acta Radiol **57**: 271-278, 2016.

18. Lee SS, Lee Y, Kim N, et al. Hepatic fat quantification using chemical shift MRI and MR spectroscopy in the presence of hepatic iron deposition: validation in phantoms and in patients with chronic liver disease. J Magn Reson Imaging **33**: 1390-1398, 2011.

19. Shimizu K, Namimoto T, Nakagawa M, et al. Hepatic fat quantification using automated six-point Dixon: comparison with conventional chemical shift based sequences and computed tomography. Clin Imaging **45**: 111-117, 2017.

20. Imajo K, Kessoku T, Honda Y, et al. Magnetic resonance imaging more accurately classifies steatosis and fibrosis in patients with nonalcoholic fatty liver disease than transient elastography. Gastroenterology **150**: 626-637.e627, 2016.

21. Tomeno W, Yoneda M, Imajo K, et al. Evaluation of the liver fibrosis index calculated by using real-time tissue elastography for the non-invasive assessment of liver fibrosis in chronic liver diseases. Hepatol Res **43**: 735-742, 2013.

22. Sumida Y, Yoneda M, Hyogo H, et al. A simple clinical scoring system using ferritin, fasting insulin, and type IV collagen 7S for predicting steatohepatitis in nonalcoholic fatty liver disease. J Gastroenterol **46**: 257-268, 2011.

23. Loomba R, Wolfson T, Ang B, et al. Magnetic resonance elastography predicts advanced fibrosis in patients with nonalcoholic fatty liver disease: a prospective study. Hepatology (Baltimore, Md) **60**: 1920-1928, 2014.

24. Baracos V, Kazemi-Bajestani SM. Clinical outcomes related to muscle mass in humans with cancer and catabolic illnesses. Int J Biochem Cell Biol **45**: 2302-2308, 2013.

25. Prado CM, Lieffers JR, McCargar LJ, et al. Prevalence and clinical implications of sarcopenic obesity in patients with solid tumours of the respiratory and gastrointestinal tracts: a population-based study. Lancet Oncol **9**: 629-635, 2008.

26. Shen W, Punyanitya M, Wang Z, et al. Total body skeletal muscle and adipose tissue volumes: estimation from a single abdominal cross-sectional image. J Appl Physiol (1985) **97**: 2333-2338, 2004.

27. Belfort R, Harrison SA, Brown K, et al. A placebo-controlled trial of pioglitazone in subjects with nonalcoholic steatohepatitis. The N Engl J Med **355**: 2297-2307, 2006.

28. Xing B, Zhao Y, Dong B, Zhou Y, Lv W, Zhao W. Effects of sodium-glucose cotransporter 2 inhibitors on non-alcoholic fatty liver disease in patients with type 2 diabetes: a meta-analysis of randomized controlled trials. J Diabetes Investig **11**: 1238-1247, 2020.

29. Sattar N, Fitchett D, Hantel S, George JT, Zinman B. Empagliflozin is associated with improvements in liver enzymes potentially consistent with reductions in liver fat: results from randomised trials including the EMPA-REG OUTCOME® trial. Diabetologia **61**: 2155-2163, 2018.

30. Komiya C, Tsuchiya K, Shiba K, et al. Ipragliflozin improves hepatic steatosis in obese mice and liver dysfunction in type 2 diabetic patients irrespective of body weight reduction. PloS One **11**: e0151511, 2016.

31. Koike Y, Shirabe SI, Maeda H, et al. Effect of canagliflozin on the overall clinical state including insulin resistance in Japanese patients with type 2 diabetes mellitus. Diabetes Res Clin Pract **149**: 140-146, 2019.

32. Yamashita H, Takenoshita M, Sakurai M, et al. A glucose-responsive transcription factor that regulates carbohydrate metabolism in the liver. Proc Natl Acad Sci U S A **98**: 9116-9121, 2001.

33. Ferré P, Foufelle F. Hepatic steatosis: a role for de novo lipogenesis and the transcription factor SREBP-1c. Diabetes Obes Metab **12** (Suppl 2): 83-92, 2010.

34. Liu G, Li Y, Hu P, Cheng D, Shi H. The combined effects of serum lipids, BMI, and fatty liver on 18F-FDG uptake in the liver in a large population from China: an 18F-FDG-PET/CT study. Nucl Med Commun **36**: 709-716, 2015.

35. Kamimura K, Nagamachi S, Wakamatsu H, et al. Associations between liver (18)F fluoro-2-deoxy-D-glucose accumulation and various clinical parameters in a Japanese population: influence of the metabolic syndrome. Ann Nucl Med **24**: 157-161, 2010.

36. Sha S, Polidori D, Heise T, et al. Effect of the sodium glucose cotransporter 2 inhibitor canagliflozin on plasma volume in patients with type 2 diabetes mellitus. Diabetes, obesity & metabolism **16**: 1087-1095, 2014.